PLASMA DIAGNOSTICS

TRENDS AND ADVANCES IN P–11B SYNTHESIS RESEARCH (REVIEW)

© 2025 E. G. Vovkivsky, A. Yu. Chirkov*

Bauman Moscow State Technical University, Moscow, Russia

**e-mail: chirkov@bmstu.ru*

Received December 11, 2024

Revised January 07, 2025

Accepted January 15, 2025

Abstract. The possible use of the neutronless p–11B reaction is of potential interest from the point of view of obtaining clean energy. Modern studies for various schemes for implementing this reaction are considered, estimates of the maximum energy gain in plasma for various system parameters are presented. Possibilities of increasing the reaction rate compared to Maxwellian plasma are discussed. The effect of alpha particle accumulation and possible ways of reducing it are analyzed.

Keywords: *p–11B reaction, neutronless thermonuclear fusion, energy balance, reaction rate, alpha particle yield*

DOI: 10.31857/S03672921250109e9

1. INTRODUCTION

Despite the long history of thermonuclear research, the relevance of the analysis of various schemes for using the energy of nuclear fusion reactions is still high. Currently, there is renewed interest in neutronless p–^{11}B-reaction, which is attractive from the point of view of the potential possibility of using thermonuclear fusion to produce electricity and other forms of energy, as well as non-energy applications [1]. The interaction between a proton and a boron-11 nucleus results in the following transformation:

$$p + {}^{11}B \rightarrow 3\alpha + 8.68 \text{ МэВ}, \quad (1)$$

where p is a proton,^{11}B is the boron-11 nucleus,α— alpha particle.

Research on the capabilities of the p– ^{11} B reaction began about 50 years ago (1970s) [2–5], with the main conclusions from early works remaining relevant to this day. The reaction rate of p–

^{11}B in plasma is relatively low even at very high temperatures (T > 100 keV) [6]. Energy balance studies clearly show that at such high temperatures, the losses due to bremsstrahlung radiation are practically equal to or exceed the energy released [2–5, 7, 8]. For the same reason, considering a system with a strong magnetic field in low-density plasma apparently has no practical significance, as radiation losses are even greater due to cyclotron radiation.

Currently, there is a greatly increased interest in finding possible ways for practical utilization of the energy from the p– ^{11}B reaction [9, 10]. In modern research, the greatest hopes are placed on fast-occurring processes with the formation of high-density plasma [11]. Low-density plasma under stationary or quasi-stationary conditions is also being considered [12–15].

2. FEATURES OF THE p – ^{11}B REACTION

It should be noted that from a nuclear physics perspective, the p– ^{11}B reaction is of significant interest, especially its mechanism [16–18]. Also under investigation are the cross-section and reaction rate, the influence of polarization of reacting nuclei, excitation of secondary reactions, and other issues [19–27].

At relatively low energies, reaction (1) is described by the compound nucleus mechanism of ^{12}C* with an excited state energy of 15.96 MeV [17]. Direct decay with the immediate formation of three α -particles is possible. But a two-stage transformation is more likely. In the first stage, a ^{8}Be nucleus may form in its ground unexcited state:

$$\mathrm{p} + {}^{11}\mathrm{B} \rightarrow {}^{8}\mathrm{Be} + \alpha_0. \qquad (2)$$

Here, the energy of the α -particle $E_{\alpha 0} \sim 6$ MeV.

The main channel, the scheme of which is shown in Fig. 1, corresponds to the formation of the nucleus ^{8}Be* in the first excited state with its subsequent decay:

$$p + {}^{11}\mathrm{B} \rightarrow {}^{8}\mathrm{Be}^{*} + \alpha_1, \qquad (3)$$

$$^{8}\mathrm{Be}^{*} \rightarrow \alpha_2 + \alpha_2. \qquad (4)$$

A total of 8.68 MeV is released in the reaction $p + {}^{11}\mathrm{B} \rightarrow 3\,\alpha$If reactions (3) and (4) are considered independently, then the energy of the alpha particle in reaction (3) should be $E_{\alpha 1} \sim 4$ MeV, the energy of each alpha particle in reaction (4) should be $E_{\alpha 2} \sim 2.3$ MeV. Since the decay of the

excited nucleus ^{8}Be* occurs in a very short time (~ 10^{-16} s), during which α_1 and two particles α_2 are under the influence of mutual nuclear forces, in experiments the spectrum of alpha particles has a maximum in the energy range of 3.5–5 MeV and a wide range at energies < 3.5 MeV [23]. Fig. 2 shows the calculated spectrum [23], which corresponds to the spectra obtained experimentally [26].

The energy spectrum of α -particles is important for the energy balance of thermonuclear plasma, since the energy of α -particles determines the fraction of energy transferred to the ion and electron components of the plasma. A favorable regime can be implemented if the alpha particles transfer almost all their energy to the ions. This maintains a high ion temperature necessary for a high reaction rate, while the electron temperature is minimal, and, consequently, radiation losses are minimal.

Note that the following reactions can also proceed in parallel with those considered above [6, 17]:

$$p + {}^{11}\mathrm{B} \rightarrow {}^{12}\mathrm{C} + \gamma + 16.0 \text{ МэВ}, \quad (5)$$

$$p + {}^{11}\mathrm{B} \rightarrow {}^{11}\mathrm{C} + n - 2.76 \text{ МэВ}. \quad (6)$$

At relatively low energies, the cross-sections of reactions (5) and (6) are much smaller than the cross-section of the main reaction (2)-(4). As the energy of incident protons increases to $E_p \sim 4$ MeV, the cross-section of reaction (6) becomes approximately equal in magnitude to the cross-section of the main reaction. Reaction rates and product yields are determined by the reaction rate parameter $\langle \sigma v \rangle$ (the product of the reaction cross-section and the relative velocity of colliding particles averaged over distribution functions), therefore it is precisely the ratio of these values that determines the yield fraction realized in the corresponding reactions. Using data [6], it can be estimated that in the most important ion temperature range T_i = 200-500 keV, the ratios of the rate parameters of reactions (5) and (6) to the rate parameter of the main reaction are ~ 10^{-4} and < $3 \cdot 10^{-3}$ respectively.

High-energy α -particles can interact with ^{11}B nuclei

$$^{4}\mathrm{He} + {}^{11}\mathrm{B} \rightarrow {}^{14}\mathrm{C} + p + 0.783 \text{ МэВ}, \quad (7)$$

$$^{4}\mathrm{He} + {}^{11}\mathrm{B} \rightarrow {}^{14}\mathrm{N} + n + 0.157 \text{ МэВ}, \quad (8)$$

The cross-sections of these secondary reactions become approximately equal to the cross-section of the main reaction at incident alpha particle energies $E_\alpha \sim 3$ MeV. At $T_i \sim 300$ keV, the ratios of the rate parameters of reactions (7) and (8) to the rate parameter of the main reaction are $\sim 5 \cdot 10^{-4}$ and $\sim 2 \cdot 10^{-2}$ respectively.

In the case of significant accumulation of alpha particles in the plasma, the yield of reaction products (8) may be noticeable. Therefore, the question of neutron yield in this reaction deserves attention. According to data [6], at energies $E > 3$ MeV, the cross-section of reaction (8) is comparable to the cross-section of the main reaction (1). However, the probability that such a fast particle will react before slowing down is small. An estimate based on the values of particle velocity and cross-section gives a characteristic time required for the particle reaction, which is approximately two orders of magnitude greater than the time of its deceleration. The rate of reaction (8) in plasma with a temperature of several hundred keV is two orders of magnitude less than the rate of the main reaction. Therefore, the neutron yield apparently does not exceed 1% of the alpha particle yield. Considering the relatively small amount of energy output in reaction (8), the share of energy output in neutrons can be estimated at the level of ~0.05%.

It should be noted that if the fuel contains an impurity of isotope ^{10}B, in addition to the indicated parallel and secondary reactions, reactions involving this isotope can occur in the plasma, but we do not consider such reactions here. Taking into account both the reaction rates and the energy released in each of the reactions (1)-(8), neutrons and radioactive products constitute less than 1% of the energy output. Therefore, the p-^{11}B fuel cycle is usually called aneutronic, although, as can be seen from the above estimates, some insignificant level of radioactivity is not excluded.

Recently, data on the cross-section and reaction rate have been updated [21]. Due to the low rate of energy release in thermonuclear p-^{11}B plasma and its practical equality to bremsstrahlung losses, even a relatively small increase in the reaction cross-section can significantly improve the energy balance. A new analysis of the data on the p-^{11}B reaction cross-section in [21] showed significantly higher values in the energy range > 500 keV compared to the data of the previous analysis [19]. In particular, at the energy of incident protons $E_p = 520$ keV, the cross-section was approximately 12% higher.

Figure 3 shows the reaction cross sections according to the "new" [21] and "old" [19] data. Figure 4 presents a comparison of reaction rate data for Maxwellian distributions of reacting ions. Note that the reaction rate parameter calculated by numerical integration of the cross section [19]

and based on the approximating functions given in [19] shows values differing within 5% in the range of 250-500 keV.

The presented dependence of the reaction rate parameter corresponds to Maxwellian distributions of ions of both types having the same temperature T_i. It should be noted that in a magnetic field for polarized nuclei, whose spins are oriented in a specific way relative to the magnetic induction vector, the cross section of the p-^{11}B reaction is 1.6 times higher [22]. Methods for producing polarized particle beams have been developed today. However, it is currently difficult to judge the technical possibilities of achieving a high degree of polarization of thermonuclear fuel under conditions of specific systems, as well as how quickly relaxation will occur. Therefore, we do not consider the polarization effect here.

3. CURRENT RESEARCH

3.1. Laser Systems: Experiments

For the first time in the world, the p-^{11}B reaction was initiated in laser plasma at the "Neodim" facility (Korolev, Russia) in 2005 [28]. Later, the yield of thermonuclear alpha particles as a result of the interaction of protons and boron was achieved in experiments in laser plasma [29-36]. Experiments demonstrate that laser systems with various parameters generate a significant yield of alpha particles.

Table 1 presents the parameters of laser systems: wavelength λ; intensity I of laser radiation; energy E and pulse time τ; density of the formed plasma (n_e — electron density, n_B — boron density). Characteristic energies, yield parameters, and features of the alpha particle spectrum are provided.

3.2. Laser system s: theory

Currently developed laser schemes for D-T reaction do not allow their application to create conditions necessary for effective p-^{11}B fusion. For 40 years, various schemes have been proposed, the main task of which was to reduce the energy spent on fuel ignition [37-39]. For example, in [39], a method of "igniting" solid p-^{11}B fuel using a picosecond laser is considered. Estimates show that a pre-pulse with a duration within a picosecond avoids the generation of a relativistic plasma cloud at the leading edge of beam propagation and reduces the "ignition" temperature T_{ign}

. For this method, threshold values of energy flux density and temperature are determined to be $W = (1\text{-}2)\cdot 10^{9}$ J $\cdot$cm $^{-2}$, $T_{ign} = 87$ keV, respectively.

Based on the high yield of α-particles obtained in experiments [31, 32], a theory of quasi-chain reaction involving protons of resonant energy was proposed [40, 41]. However, computational analysis did not confirm the initial optimism regarding the effect of quasi-chain reaction [42-46].

As a variant of reactor implementation, a magneto-inertial scheme in a configuration with Helmholtz coils was proposed [47]. The coils are powered by the energy of a capacitor charged by a laser pulse. In such a scheme, fields of level B = 1 kT were experimentally obtained at laser radiation intensity $I = 5 \cdot 10^{16}$ W/cm ^{2} [48]. The amplitude of the field in the mentioned experiments increased approximately proportionally to the intensity of laser radiation.

Technologies for generating ultrashort laser pulses of high intensity and frequency have opened new possibilities for improving the efficiency of laser systems. The results of numerical modeling of the process of attosecond laser pulse impact on a target show that ions acquire radial acceleration and are accelerated to an energy of ~ 600 keV, corresponding to the maximum cross-section of the p– ^{11}B reaction [49, 50]. Problems of converting laser energy into the energy of ions accelerated by a picosecond laser pulse are considered [51–53]. This includes analyzing the possibilities of developing collective ion acceleration schemes [54] and laser-plasma sources of high-energy ions [55, 56].

3.3. Magnetic confinement

It should be noted that recently the first measurements of alpha particle yield in a magnetic confinement system – the LHD stellarator [57] – were conducted. Speaking about the prospects of a reactor with magnetic confinement, it is worth noting the difficulty of achieving the conditions necessary for fusion reaction in these systems, namely high confinement time and high (for magnetic systems) fuel density. In addition, the presence of a strong magnetic field in the plasma leads to additional losses due to cyclotron radiation. In this case, an increase in the reaction rate can be caused by the counter-movement of fuel components with high relative velocity.

Similar concepts with beam-plasma fusion were proposed in the CBFR reactor system designs [58] and centrifugal trap [59]. In these concepts, the kinetic energy of the relative motion of the p– ^{11}B mixture components corresponds to the energy of colliding nuclei in the center of

mass system $E \approx 680$ keV, at which the reaction cross-section is maximum. Therefore, this approach was designated by the authors as "resonant fusion." However, from the perspective of energy balance, taking into account all processes in such non-equilibrium plasma, and especially considering relaxation [60], many questions remain about the feasibility of such approaches.

As a recent study [15] has shown, taking into account refined data on the reaction cross-section, the characteristic temperatures at which maximum enhancement Q is achieved in a stationary system are $T_i \approx 300$ keV and $T_e \approx 120$ keV. The difference between ion and electron temperatures was determined by considering the energy balance of ions and electrons. At these temperatures, almost all the energy of alpha particles formed in the reaction is transferred to ions, with alpha particles transferring ~5% of their energy to electrons during deceleration. If the equilibrium content of thermalized alpha particles is not taken into account (considering only their fast population), the enhancement can reach a value of $Q > 10$. This result is more optimistic than the previous estimate [8], according to which the enhancement is limited to a value of $Q \approx 4$. The characteristic value of the product $n_p \tau \approx 1.5 \cdot 10^{22}$ m$^{-3} \cdot$ s (n_p is the proton density, τ is the plasma confinement time). Taking into account the thermalized population of alpha particles, $Q < 1$. Therefore, the implementation of a stationary scenario requires the development of effective methods for removing thermal alpha particles. It should also be noted that these results correspond to radiation losses only due to bremsstrahlung; consequently, for magnetic confinement systems with low β (β is the ratio of plasma pressure to magnetic pressure), taking into account cyclotron radiation will lead to the fundamental impossibility of high values of Q.

In work [61], for low-density plasma characteristic of magnetic confinement systems, possibilities of heating components to temperatures corresponding to resonant energies at which the reaction cross-section sharply increases are considered. The first resonance of the p–^{11}B reaction cross-section corresponds to an energy in the center-of-mass system of 163 keV, with a resonance width of about 5 keV. The second resonance is characterized by an energy of 675 keV, with a width of ~300 keV. Heating to such high temperatures can potentially be realized by thermonuclear alpha particles during their avalanche formation. For a density of $n \sim 10^{20}$ m^{-3}, estimates show the possibility of "ignition" (thermonuclear power P_{fus} exceeds the power loss due to bremsstrahlung P_{br}) at an initial component temperature of $T_0 = 200$ keV and a ratio of boron to proton nuclei concentrations $n_B / n_p < 0.1$. It is assumed that the avalanche effect can be realized

when the density of alpha particles is comparable to the density of fuel components, making the reaction self-sustaining.

In work [62], the concept of a thermonuclear propulsion system with p– ^{11}B fuel based on an open magnetic trap with centrifugal confinement is considered. Such a system with a thermonuclear power level of ~10^{5} W/m^{2} requires electric fields of ~350 MV/m and magnetic fields of ~ 30 T. It should be noted that in this work, radiation conversion is also discussed.

Note that there are works that consider a tokamak using p- ^{11}B fuel. For example, in a recent paper [63], an analysis of parameters needed to achieve amplification Q = 30 was performed for a spherical tokamak with an aspect ratio A = 1.7. From a physics perspective, the most unfeasible requirement at present appears to be increasing the p- ^{11}B reaction rate by 5 times at a volume-averaged plasma temperature of T = 33 keV. If we assume that such an increase is possible, then according to [63], the thermonuclear power of such a reactor would be 107 MW. At the same time, other technical parameters of the reactor generally correspond to the current level of spherical tokamaks.

3.4. Inertial-electrostatic confinement, oscillating plasma

For systems with inertial-electrostatic plasma confinement, the required system parameters turned out to be extremely strict [64]. In traditional inertial electrostatic confinement schemes, there are difficulties in obtaining high power gain due to Coulomb collisions. Therefore, as a development of the inertial-electrostatic confinement approach, possible regimes of oscillating plasma in various schemes are being investigated.

In the concept of a periodically oscillating plasma sphere [65, 66], it is assumed to maintain a non-equilibrium state of the plasma. An injected electron beam creates a potential well that accelerates ions, causing them to oscillate. In this case, counter-collisions of ions lead to fusion reactions. Experiments in a nanosecond vacuum discharge of low energy (1-2 J) with a virtual cathode showed a total yield of α-particles Y_{α}=10 particles/ns.

A scheme of oscillation of oppositely charged ions has also been proposed to form a neutral and at the same time stable system with high-frequency oscillations [67].

3.5. Inertial and magneto-inertial confinement

The NIF laser facility has achieved ignition parameters in the mode of inertial confinement of D-T plasma [68]. Similar parameters can be implemented in a Z-machine with a magnetized load [69], especially after upgrading. In the case of strong magnetic fields, the expansion time increases by about an order of magnitude compared to the purely inertial case, and, consequently, the density requirements are reduced.

In the MAGO-MTF system [70], the target compression is carried out by a driver in the form of a wire array through which current is passed. The evaporating wires emit radiation, which also has a compressing effect on the target.

The implementation of ignition conditions for the p- ^{11}B reaction in inertial systems with high-density plasma [71] is proposed using a proton beam with energy $E_p = 2.5$ MeV, acting on a target pre-compressed to a density of $\rho = 4000$ g/cm^3 ($\rho R \approx 8.5$ g/cm^2), and also heated to temperatures $T_i = 220$ keV, $T_e = 85$ keV. These parameters are achievable for the target during the final stage of "hot spot" heating. At the early heating stage ($T \sim 10$ keV), the use of a beam with energy $E_p \sim 200$ MeV is assumed. Possibly, in magneto-inertial systems, the conditions necessary for highly efficient p- ^{11}B fusion are easier to fulfill [72].

Parameter estimates for the ICF scheme with fast ignition of p- ^{11}B fuel by a proton beam with energy of 1 MeV [73] show the possibility of ignition with the formation of "hot spots" at the beam penetration depth of 2.5 μm. In this case, the inertial confinement parameter $\rho R = 12$ g/cm^2. It is potentially possible to reduce this value to the level of $\rho R = 1$ g/cm^2 in a magneto-inertial scheme [74]. We emphasize that for magneto-inertial fusion, the plasma decay time depends on the method of magnetic field generation and, as a rule, it significantly exceeds the time of inertial expansion.

Analyzing the above, it can be concluded that systems with high-density plasma appear more promising compared to systems with stationary confinement of low-density plasma in a magnetic field. At high densities, in particular, the Coulomb logarithm decreases, and, consequently, the rate of energy transfer from ions to electrons also decreases. Extremely high-density plasma is created in inertial fusion facilities, which can operate only in pulsed mode. On the one hand, this is in a certain sense their disadvantage, associated with the costs of compression and heating of the initial plasma. On the other hand, in such systems, the content of products can be reduced with a certain

organization of the working process. This means that the plasma can be cleaner, and, therefore, radiation losses can be reduced.

3.6. Plasma focus, Z-pinches

Comparing estimates for magnetic confinement systems and laser inertial systems, it can be stated that in the latter case, the conditions for effective implementation of fusion in the p– ^{11}B reaction seem to be feasible, despite the requirements for ultra-high densities. The magnetic field in pulsed inertial systems increases the lifetime of the plasma formation compared to the time of its purely inertial expansion, which reduces the requirements for plasma density. Such conditions can be realized in dense plasma focus (DPF) devices [75]. Therefore, DPF is considered as a concept for a p– ^{11}B reactor. Estimates show the possibility of compressing p– ^{11}B plasma to ultra-high density ($n \sim 10^{30}$–10^{31} m^{-3}) and heating it to the required temperature [76–80].

Note that the discharge in a plasma focus is attributed to the so-called non-cylindrical Z-pinches. Plasma focus devices consist of concentric electrodes enclosed in a vacuum chamber. At the moment of the pulse, the gas is ionized and a current sheath is formed, consisting of current filaments that move toward the end of the inner electrode (anode). Upon reaching the inner electrode, they converge, forming a dense magnetized plasmoid. At this moment, additional energy or matter input is possible. The implementation of thermonuclear conditions involves the use of plasma compression instability to concentrate energy in the plasmoid. The yield of reaction products (for example, neutrons when using deuterium load) in experiments with small currents $I \sim 1$ MA is proportional to I^4, however, when the current (and plasma density) increases, the yield of products does not grow according to such a strong dependence. The paper [80], discussing the prospects of p– ^{11}B fusion on a plasma focus device, in particular, provides a neutron yield value of $\sim 2.5 \cdot 10^{11}$ for a discharge in deuterium. The released energy is ~0.2 J, with an input energy of 60 kJ. Importantly, even in a device with such low energetics, ions with energies of ~240 keV were detected. It should be emphasized that Z-pinches are characterized by the formation of high-energy ions (~1 MeV and more) [81, 82], which is of interest from the perspective of the p– ^{11}B reaction, the rate of which has a maximum at an energy of ~600 keV.

In experiments with powerful cylindrical Z-pinches, significant progress has also been achieved. For example, the lifetime of the pinch has been substantially increased due to its stabilization by creating a radial gradient of axial flow velocity of the accelerated plasma [83, 84].

In the mentioned experiments, the working gas is deuterium, with electron density and temperature reaching values of $n_e \approx 10^{17}$ cm^{-3} and $T_e \approx T_i \approx 1$ keV respectively.

In X-pinches (a special case of Z-pinch with a solid load of crossed wires), the formation of a constriction is accompanied by the appearance of a so-called hot spot (one or several), in which, as assumed, conditions necessary for thermonuclear fusion can be realized, including as a result of radiation collapse [85].

The maximum plasma density and temperature are achieved at the final stage of pinch constriction compression. The processes that determine the duration of this phase preceding the pinch destruction are apparently associated with the development of turbulence and energy dissipation [86, 87].

Analysis of neutron yield from D–T and D–D plasma [88] showed that a significant increase in ion energies during Z-pinch compression contributes to intensive neutron generation at the final stage of constriction compression. Estimates of Z-pinch thermonuclear plasma parameters performed in [89] show that when using D–T fuel, an enhancement $Q \sim 100$ can be achieved with a current $I = 200$ MA and initial plasma energy $W_0 = 30$ MJ, in the case of D–D plasma $Q \sim 20$ at $I = 4.5$ GA, $W_0 = 75$ GJ. Extrapolation of these results to the case of p–^{11}B plasma leads to even higher required parameters.

3.7. Degenerate plasma

As a possible way to reduce energy transfer from ions to electrons, conditions of component interaction in degenerate p–^{11}B plasma are considered [90–92]. The idea of this approach is to reduce electron-ion collisions and the corresponding Coulomb logarithm [93, 94]. The effect of electron quantization in a strong magnetic field is also considered, which also reduces the collision effect. However, to ensure the parameters of a system with degenerate plasma, it is necessary to compress the fuel to an ultra-dense state ($n \sim 10^{28}$ cm^{-3}). In [91], calculated estimates of enhancement for the p–^{11}B reaction were carried out, the value of which did not exceed 20, which, according to the authors, is a low indicator in terms of the energy balance of the reactor. The possibility of applying this effect requires additional research.

Note that at ultrahigh densities, partial "trapping" of bremsstrahlung radiation is also possible. However, for this, the plasma dimensions must be quite large. Since for the conditions of p–^{11}B fusion, the electron temperature is high ($T_e > 100$ keV), relativistic effects lead to an

additional effect of increasing bremsstrahlung radiation compared to its growth according to the non-relativistic law ($\propto T_e^{1/2}$) [95].

4. POSSIBLE SCENARIOS, PROBLEMS AND WAYS OF IMPROVEMENT

4.1. Energy Balance and Maximum Gain

Regardless of the system type and its operation mode (stationary or pulsed), the energy gain coefficient in the plasma can be represented as

$$Q = \frac{W_{fus}}{W_{in}}, \tag{9}$$

where W_{fus} is the fusion energy released over a certain time, W_{in} is the energy input into the plasma.

The composition of p– ^{11}B fuel will be characterized by the ratio

$$x_{\mathrm{B}} = \frac{N_{\mathrm{B}}}{N_p} = \frac{n_{\mathrm{B}}}{n_p}, \tag{10}$$

where N_p and N_{B} are the numbers of particles of each component, protons and boron-11 nuclei, respectively, n_p and n_{B} are the densities (concentrations) of the components.

The plasma energy balance in the simplest case can be represented as

$$\frac{dW_p}{dt} = P_{fus} + P_{ext} - P_{rad} - \frac{W_p}{\tau}, \tag{11}$$

Here

$$P_{fus} = n_p n_{\mathrm{B}} \langle \sigma v \rangle E_{fus} V = x_{\mathrm{B}} n_p^2 \langle \sigma v \rangle E_{fus} V \tag{12}$$

is the thermonuclear power, E_{fus} is the energy output in the reaction, V is the plasma volume, P_{ext} is the external heating power, P_{rad} is the radiation loss, t is time,

$$W_p = \frac{3}{2}(n_p + n_{\mathrm{B}}) k_B T_i V + \frac{3}{2} n_e k_B T_e V = \frac{3}{2} n_p k_B T_i \left[\left(1 + x_{\mathrm{B}} + \frac{T_e}{T_i} \right)(1 + 5x_{\mathrm{B}}) \right] V \tag{13}$$

is the plasma energy, k_B is the Boltzmann constant, T_i is the ion temperature, T_e is the electron temperature, τ is the particle (energy) confinement time.

Note that we do not consider spatial distributions of parameters here. Using temperature in the expression for plasma energy implies that plasma components have Maxwellian distributions. Otherwise, temperature can be understood as an effective value characterizing the average energy of particles. The energy balance in the form of (11) can be considered both for stationary conditions ($dW_p / dt = 0$), characteristic of magnetic confinement, and for inertial systems ($dW_p / dt \neq 0$). In the latter case, the power P_{ext} of external heating accounts for energy input during compression.

In a Maxwellian plasma with $T_e = T_i$, even if radiation losses are associated only with bremsstrahlung (and no other mechanisms), they exceed thermonuclear power at virtually any temperature. Therefore, it is necessary to account for the difference in values of T_e and T_i. For this, let's consider the energy balance of ions and electrons separately:

$$\frac{dW_i}{dt} = \alpha_i P_{fus} + \delta_i P_{ext} - P_{ie} - \frac{W_i}{\tau}, \tag{14}$$

$$\frac{dW_e}{dt} = \alpha_e P_{fus} + \delta_e P_{ext} + P_{ie} - P_{rad} - \frac{W_e}{\tau}, \tag{15}$$

where $W_e = 3n_i k_B T_i V / 2$ and $W_e = 3n_e k_B T_e V / 2$ are the energies of ions and electrons respectively; α_i and α_e — portions of energy from thermonuclear α -particles transferred to ions and electrons; δ_i and δ_e — portions of external energy transferred to ions and electrons; P_{ie} — power of energy exchange during collisions between ions and electrons.

The power transferred from ions to electrons, [3]

$$P_{ie} = \frac{3}{2}\left(\frac{n_p}{\tau_{pe}} + \frac{n_B}{\tau_{Be}}\right) k_B (T_i - T_e), \tag{16}$$

where

$$\tau_{ie} = \frac{3\pi\sqrt{2\pi}\varepsilon_0^2 m_i m_e}{Z_i^2 e^4 n_i \ln\Lambda_{ie}} \left(\frac{k_B T_e}{m_e}\right)^{3/2} \tag{17}$$

— the time of Coulomb collisions of ions with electrons; ε_0 — electric constant; e — electron charge; m_e — electron mass; $i = p$, B — ion type; m_i and Z_i — mass and charge of the ion; $\ln \Lambda_{ie}$ — Coulomb logarithm.

In the intensive combustion mode, the main components in (14), (15) are associated with thermonuclear energy release, radiation, and energy exchange between ions and electrons. At high electron temperatures, characteristic of p– ^{11}B fusion, thermonuclear – particles transfer their energy mainly to ions (this issue is discussed in more detail in Section 4.3). At $T_e > 100$ keV, electrons are strongly cooled due to radiation ($T_e < T_i$), their temperature is maintained mainly by energy transfer from ions. Therefore, the values of P_{fus}, P_{rad} and P_{ie} are of the same order.

From the perspective of radiation losses, the electron temperature T_e should be as low as possible. However, as T_e decreases, the Coulomb collision time strongly decreases, and, consequently, the intensity of ion cooling on electrons increases. At relatively low temperatures $T_e < 50$ keV, the difference between T_e and T_i is insignificant [96], i.e., $T_e \text{ H } T_i$. Since the collision time (17) increases strongly with temperature, at $T_e \sim 150$ keV, a significant temperature difference $(T_i - T_e) \sim T_e$ is necessary for energy transfer from ions to electrons ($P_{ie} \sim P_{fus} \sim P_{rad}$). The ratio $T_e / T_i \sim 0.5$ is in some sense typical for the energy balance of thermonuclear p– ^{11}B plasma. Of course, in specific systems, especially under highly non-stationary conditions, this ratio may differ depending on the regimes. In particular, this issue is considered in [3], as well as in the comments [96] to the article on the concept of p– ^{11}B fusion in a spherical tokamak [63].

Let's consider the p– ^{11}B reaction under the following conditions: $T_i \sim 300$ keV, $T_e \sim 150$ keV, $x_B \sim 0.2$. If the confinement time τ is of the order of the characteristic fuel (boron) burnup time $\tau_{burn} = (n_p \langle \sigma v \rangle)^{-1}$, then plasma losses (the last terms in (14), (15)) compared to P_{fus} are small, as they are characterized by energy $3k_B T_i (1 + x_B + (T_e / T_i)(1 + 5x_B)) / 2 \sim 1$ MeV, which is significantly less than the energy ~ 8.7 MeV released in the p– ^{11}B reaction. For effective fuel burnup, confinement must be longer, and, consequently, plasma losses in this case are even less significant from the energy balance perspective. Note that under the specified conditions $\tau_{ie} / \tau_{burn} \sim 0.1$ and $P_{ie} \sim P_{fus}$.

Burning will not decay if $P_{br} < P_{fus}$ (P_{br} — bremsstrahlung radiation power). Bremsstrahlung radiation increases with temperature, but its growth is also largely associated with the accumulation of thermonuclear alpha particles in the plasma, the content of which $x_\alpha = n_\alpha / n_p$ (n_α — alpha particle density), according to particle balance estimates, reaches a value of $x_\alpha \sim 0.5$ [15]. Note that for the case of pure plasma ($x_\alpha = 0$) taking into account $T_e < T_i$, the energy balance allows

ignition at $T_i \approx$ 300–400 keV, and regimes with $Q > 10$ require limiting the alpha particle content at the level of $x_\alpha \sim 0.1$.

Let's consider pulsed regimes in which energy is expended only on creating the initial high-temperature plasma and its ignition. At the burning stage, energy is not supplied, although matter may enter the reaction zone to partially compensate for the burned fuel. In such regimes, the energy supplied to the plasma W_{in} is the energy of the plasma with initial parameters (at time $t = 0$).

If the substance does not enter the reaction zone, then the energy gain coefficient in the plasma can be represented as follows:

$$Q = \xi \frac{x_B E_{fus}}{(1+x_B)E_i + (1+5x_B)E_e}, \tag{18}$$

where ξ — fuel burn-up completeness; E_i and E_e — energies supplied from the driver per ion and electron, respectively; x_B characterizes the initial fuel composition.

The burn-up completeness ξ when $x_B < 1$ is defined as the ratio of the number of burned boron nuclei $(N_B)_{burn}$ to the total number of boron nuclei $(N_B)_{tot}$ introduced into the reaction volume,

$$\xi = \frac{(N_B)_{burn}}{(N_B)_{tot}} = \frac{1}{(N_B)_{tot}} \iint n_B n_p \langle \sigma v \rangle dV dt. \tag{19}$$

Here, the time integration t is carried out from the conditional beginning of the reaction ($t = 0$) over the time interval t_R until the end of the reaction process. Note that the end of the reaction is determined by the attenuation of the reaction due to the depletion of one fuel component (boron), plasma decay, and other factors depending on the specific scenario under consideration. We consider a zero-dimensional approximation, whereby integration over the reaction volume V is trivial. In general, the densities of protons n_p and boron nuclei n_B, as well as the reaction volume V in formula (18) may depend on time.

As can be seen from (18), high gain ($Q > 10$) is achievable if the driver initiates combustion with small energy expenditure, i.e. $E_i \ll k_B T_i$, $E_e \ll k_B T_e$, where T_i and T_e — temperature values at the combustion stage. These temperatures may differ from the initial temperatures due to plasma heating by reaction products. Also note that with volumetric ignition, the relative content of alpha particles x_α increases with increasing burn-up completeness ξ.

When analyzing pulse systems with p- ^{11}B reaction, it is necessary to take into account that energy release becomes intensive at ion temperatures $T_i > 100$ keV (in Maxwellian plasma). When discussing non-Maxwellian plasma, the energies of colliding nuclei should be of the same order of magnitude. If we consider the energy invested in all components of the p- ^{11}B mixture (protons, boron nuclei, and electrons), then per particle this energy (the value in the denominator of (18)) can be ~ 1 MeV. This value is comparable to the energy output from a single reaction. According to (18) and (19), high amplification requires the following conditions: relatively low initial temperatures (energies) of plasma particles and prolonged burning (with high combustion completeness). Currently, it is difficult to predict in which type of systems these conditions can be simultaneously fulfilled.

For pulse systems, two limiting cases of thermonuclear burning initiation can be considered [97]: volumetric ignition and the thermonuclear spark mode ("hot spot"). In the first case, the entire volume of fuel must be heated to thermonuclear temperatures; in the second case, only a small part of it, and due to the released energy, the burning propagates to adjacent areas. The second option is more energy-efficient, at least for "traditional" types of thermonuclear fuel (D-T, D-D) [97]. In the case of p- ^{11}B fuel, the possibility of its implementation is not obvious due to high radiation losses, which require almost all the energy of thermonuclear α -particles to compensate. In this case, energy from the reaction initiation area is released as hard X-ray radiation, which requires ultra-high fuel density or significant fuel dimensions for absorption. Both can lead to prohibitively large energetics of the corresponding configuration. This can be easily verified, for example, based on a simple estimate of the path length [98] for X-ray photons with energies of ~ 100 keV. However, we do not provide the corresponding numerical data here, since radiation transfer in super-dense plasma is very complex, and simple estimates apparently give very rough results. We emphasize the high importance of the radiation problem for p- ^{11}B fusion.

Let's analyze the energy balance (based on equations (14), (15)) for conditions $x_B = 0.2$, $\alpha_i \approx 1$, $\alpha_e \approx 0$, no external heating ($\delta_i = 0$, $\delta_e = 0$), plasma losses are not taken into account ($W_i/\tau \approx 0$, $W_e/\tau \approx 0$). Under these conditions, the main components of the energy balance are: $P_{ie} \approx P_{fus} \approx P_{rad}$. In this case, estimates show that when $T_i > 200$ keV, $T_e > 100$ keV at the initial moment, ions can be heated ($dW_i/dt > 0$, $dT_i/dt > 0$). The characteristic reaction time τ_R (existence of the burning stage) will be determined by the intensity of cooling due to bremsstrahlung radiation. At $T_i = 200$ keV, $T_e = 100$ keV, in order of magnitude, it is comparable to the time $(n_p \langle \sigma v \rangle)^{-1}$

characterizing the burnup of boron. Assuming in formula (18) $E_i = 3\,k_B T_i/2$, $E_e = 3\,k_B T_e/2$, we estimate that $Q > 2$ if $\xi > 0.5$.

If in a certain volume of plasma the energy output can exceed the energy expenditure by more than twofold, then one can hope that the energy released in this volume will initiate the combustion process in the neighboring volume and, accordingly, its further propagation. It is hardly possible to predict the effectiveness of such a scenario within the framework of the zero-dimensional balance approach considered here. For p-^{11}B fusion, in addition to high temperatures $T_i \sim 200$ keV, $T_e \sim 100$ keV, extremely high plasma densities and a sufficiently long lifetime of the plasma formation are required: the product of plasma density and confinement time $n\tau \sim 10^{22}$ m$^{-3}\cdot$s. The problems of implementing energetically favorable p-^{11}B fusion are largely related to the reaction rate, which is sufficiently high only at high energies of the reacting nuclei. The energy of fuel particles and electrons is not small compared to the energy of the products.

4.2. Reaction rate

In general, the reaction rate parameter is calculated as a result of averaging over the velocities of reacting components

$$\langle \sigma v \rangle_{jk} = \iint \sigma(|\mathbf{v}_j - \mathbf{v}_k|)\,|\mathbf{v}_j - \mathbf{v}_k|\, f_j(\mathbf{v}_j) f_k(\mathbf{v}_k) d^3 v_j d^3 v_k. \qquad (20)$$

Here $f_j(\mathbf{v}_j)$ and $f_k(\mathbf{v}_k)$ are velocity distribution functions of the components, components *j* and *k* are protons and ^{11}B nuclei.

In the case of Maxwellian distributions with different temperatures $T_j \neq T_k$ the value of $\langle \sigma v \rangle_{jk}$ is the same as at the effective temperature of components $T_{eff} = (m_k T_j + m_j T_k)/(m_k + m_j)$, where m_j and m_k are the masses of reacting nuclei.

With distributions different from Maxwellian, the reaction rate can differ noticeably towards higher values [99-101].

Let's consider the reaction rate $\langle \sigma v \rangle$ for the case when protons and boron-11 ions have so-called shifted Maxwellian distributions, characterized by different velocities of macroscopic motion of the components . With a sufficiently high relative velocity, a significant increase in the reaction rate can be expected due to increased collision energy. In the case of shifted Maxwellian distributions, formula (16) takes the form [102]

$$\langle \sigma v \rangle = \frac{1}{w}\sqrt{\frac{2M}{\pi k_B T_i}} \exp\left(-\frac{Mw^2}{2k_B T_i}\right) \int_0^\infty \sinh\left(\frac{Muw}{k_B T_i}\right) \exp\left(\frac{Mu^2}{2k_B T_i}\right) \sigma(u) u^2 du, \qquad (21)$$

where $w = |w_j - w_k|$ is the relative hydrodynamic velocity of components, w_j and w_k are hydrodynamic velocities (flow velocities), $u = |\mathbf{v}_j - \mathbf{v}_k|$ is the relative velocity of particles, $M = m_k m_j / (m_k + m_j)$ is the reduced mass.

Figure 5 shows the dependencies of the velocity parameter of the p- ^{11}B reaction at different energies of mutual motion of components in the center of mass system $E = Mw^2/2$. As can be seen, a noticeable effect is achieved when the velocities of relative motion of components are comparable to or exceed thermal motion velocities.

A possible option for creating such strong relative flows of components can be diamagnetic drift due to a sharp pressure gradient in the presence of a magnetic field [102]. In this case, the relative velocity of protons and boron nuclei

$$w = \frac{k_B T_i}{eBL}\left(\frac{1}{Z_p} - \frac{1}{Z_B}\right), \qquad (22)$$

where B is the magnetic field induction in plasma, L is the spatial scale of pressure inhomogeneity, $Z_p = 1$ and $Z_B = 5$.

For this relative velocity to reach a value of $w \approx 10^7$ m/s, the inhomogeneity scale should be equal to $L \approx 1$ mm at an ion temperature of $T_i \approx 150$ keV and magnetic field induction in plasma $B \approx 10$ T. If the relative motion of components is caused by diamagnetic drift, it may seem that additional energy investments in the fuel components are not required. However, one should remember the need for correct accounting of the relaxation effect of spatially inhomogeneous velocity distribution and associated losses.

In principle, a similar effect of relative velocity can be achieved by injecting fast particles into the plasma. In this case, the effect may be limited by the rapid deceleration of the injected particles. A relatively small proportion of them may still have time to react before slowing down to thermal velocities. We reiterate that the effect of such an increase requires a detailed analysis of issues related to relaxation.

There are various methods for generating high-energy proton beams. For example, in experiments [103], proton beams were obtained as a result of the D–D reaction by irradiating a target of deuterated polyethylene (CD_2) with a laser pulse with energy $E \approx 600$ J, wavelength $\lambda = 1.315$ μm, and duration $\tau = 350$ ps. It was assumed that the protons were accelerated by an intense electric field. The proton energy was ~ 5.2 MeV. The results of modeling the irradiation of a boronated foil with protons of this energy predicted an alpha particle yield of $1.3 \cdot 10^{11}$ (behind the target).

4.3. Alpha particles, radiation losses

At high energies, an α-particle is decelerated mainly due to collisions with electrons. The critical energy E_c, at which the deceleration intensities on ions and electrons are equal, depends on the plasma composition and is directly proportional to the electron temperature [104, 105]. The slowing-down time τ_s characterizes the decrease in particle velocity (or kinetic energy) in plasma at energy $E > E_c$. Otherwise, $E > E_c$, the slowing-down time decreases with decreasing energy as $(E / E_c)^2 \tau_s$. According to [104], a fast particle with initial energy $E = E_c$ transfers a portion of energy $\alpha_e \approx 0.25$ to electrons.

In particular, in p– ^{11}B plasma with $x_B = 0.2$, the critical energy of α -particle equals $E_c \approx 30 \cdot k_B T_e$. At $T_e \sim$ 100–150 keV, it equals $E_c \approx$ 3–4.5 MeV. As noted in the second section, the spectrum of α-particles formed in the p– ^{11}B reaction consists of a "peak" at $E \sim 4$ MeV and a "plateau" at $E < 3.5$ MeV. Therefore, only a relatively small group of α-particles transfers > 25% of their kinetic energy to electrons. Estimates [15], assuming that fusion products form a slow-down distribution [99, 104], gave $\alpha_e < 0.05$ at $T_e > 100$ keV.

Reducing the content of thermalized α -particles has a favorable effect on increasing the amplification factor Q. However, it is currently difficult to say exactly how their removal can be organized from various systems. For magnetic confinement systems, concepts of forced α-particle removal have been proposed [106–109]. The effects of external magnetic field perturbation [107, 108] and the autoresonance mechanism [109, 110], leading to forced diffusion of α-particles of certain energies, were considered. Removal of high-energy α-particles is not advantageous from the fusion efficiency perspective, as they provide the necessary heating. In [61], calculation results are presented for low-density plasma ($n \approx 10^{20}$–10^{21} m^{-3}) in a scenario with heating due to an

"avalanche" (quasi-chain) reaction. Calculations show the possibility of ignition at an initial plasma temperature of $T = 200$ keV.

It should be emphasized that the following very important issues of p– ^{11}B fusion are associated with α-particles: ash accumulation and removal; reactions involving fast α-particles; heating of ion and electron components; possible formation of a high-energy proton population and the associated possibility of increasing the p– ^{11}B reaction rate. Obviously, all these issues require the development of a detailed kinetic model for α-particles produced in the p– ^{11}B reaction.

Increasing the average energy of plasma particles leads to more intense reactions and less intense energy exchange during Coulomb collisions. At the same time, the growth of electron temperature is accompanied by increased energy losses due to bremsstrahlung and cyclotron radiation. Quanta emitted by high-energy electrons carry away a significant amount of energy, so it is important to consider the features of the electron energy distribution. For example, calculations for distributions with a "cut-off" region of high-energy particles [111] or their redistribution to the lower energy region [112] show a noticeable reduction in radiation losses. Thus, when searching for optimal conditions, a balance must be maintained between achieving high temperatures to accelerate reactions and minimizing energy losses due to radiation.

5. CONCLUSION

The parameters of a system with p– ^{11}B fuel are subject to extremely stringent requirements. Plasma parameters exceed by orders of magnitude the requirements for "traditional" thermonuclear fuels (D–T, D–D). At the same time, achieving such parameters is accompanied by limitations associated with the accumulation of α -particles in the plasma and the need for their removal. These limitations are related to bremsstrahlung radiation and energy transfer from ions to electrons due to Coulomb collisions.

Known computational studies of non-ideal and degenerate plasma demonstrate a decrease in the Coulomb logarithm due to a more accurate description of particle interactions at high plasma densities and high magnetic fields. Quantum effects in ultra-dense degenerate plasma manifest at relatively low temperatures, so they are unlikely to improve regimes where the temperature exceeds 100 keV.

Since the main source of heating is high-energy α -particles, a more detailed simulation of their interaction with plasma components—fuel ions and electrons—is necessary. Therefore, an

important task in further research will be to simulate the kinetics of α -particles, taking into account their birth spectrum, as well as developing schemes for efficient removal of thermalized α -particles that have transferred their energy to fuel components.

The conditions necessary for the practical use of energy from the aneutronic p– ^{11}B reaction are, of course, much more difficult to achieve than for the traditional D–T reaction (and even for the D–D reaction). However, all products of the first reaction are charged, all their energy can be efficiently transferred to the plasma, and the possibility of initiating combustion with a relatively low-energy driver capable of "igniting" a small volume of plasma is potentially not excluded.

A favorable regime for efficient p11 ^{11}B fusion involves a system in which it is possible to achieve high density $n \sim 10^{30}$–10^{31} m^{-3} and ion temperature $T_i \sim 200$ keV. Systems such as Z-pinch with condensed load, in which heating occurs during rapid compression of magnetized plasma, may be promising.

REFERENCES

1. *McKenzie W., Batani D., Mehlhorn T. A., Margarone D., Belloni F., Campbell E. M., Woodruff S., Kirchhoff J., Paterson A., Pikuz S., Hora H.* // J. Fusion Energy. 2023. V. 42. P. 17. Doi: 10.1007/s10894-023-00349-9.
2. *Weaver T., Zimmerman G., Wood L*. Exotic CTR fuel: Non-thermal effects and laser fusion application. Lawrence Livermore Laboratory. California Univ. Livermore. 1973. Report UCRL-74938.
3. *Moreau D.C.* // Nuclear Fusion. 1977. V. 17. P. 13. Doi: 10.1088/0029-5515/17/1/002.
4. *Kukushkin A.B, Kogan V.I.* // Soviet J. Plasma Phys. 1979. V. 5. P. 1264. *Kukushkin A.B., Kogan V.I.* // Fizika Plazmy. 1979. V. 5. P. 1264.]
5. *McNally J.R.* // Nuclear Technol. – Fusion. 1982. V. 2. P. 9. Doi: 10.13182/FST2-1-9.
6. *Feldbacher R*. Nuclear Reaction Cross Sections and Reactivity Parameter. IAEA, 1987. https://www-nds.iaea.org/publications/nds/iaea-nds-0086/.
7. *Nevins W.M.* // J. Fusion Energy. 1998. V. 17. P. 25. Doi: 10.1023/A:1022513215080.
8. *Chirkov A.Yu* . // Yader. Fiz. Inzhiniring. 2013. V. 4. P. 1050. Doi: 10.1134/S2079562913120075. *Chirkov A.Yu* . // Nuclear Physics and Engineering. 2013. V. 4. P. 1050.]
9. 2 nd International Workshop on Proton-Boron Fusion, Rome, Italy, 5-8 September 2022. https://agenda.infn.it/event/30291/timetable/ (accessed 12.11.2024).
10. *Lerner E. J., Hassan S. M., Karamitsos-Zivkovic I., Fritsch R.* // Phys. Plasmas. 2023. V. 30. P. 120602. Doi:10.1063/5.0170216.
11. *Mehlhorn T.A*. // Phys. Plasmas. 2024. V. 31. P. 020602. Doi: 10.1063/5.0170661.
12. *Putvinski S.V., Ryutov D.D, Yushmanov P.N*. // Nuclear Fusion. 2019. V. 59. P. 076018. Doi: 10.1088/1741-4326/ab1a60.
13. *Kolmes E.J., Ochs I.E., Fisch N.J*. // Phys. Plasmas. 2022. V. 29. P. 110701. Doi: 10.1063/5.0119434.
14. *Cai J., Xie H., Li Y., Tuszewski M., Zhou H., Chen P*. // Fusion Sci. Technol. 2022. V. 78. P. 149. Doi: 10.1080/15361055.2021.1964309.
15. *Chirkov A.Yu., Kazakov K.D*. // Plasma. 2023. V. 6. P. 379. Doi: 10.3390/plasma6030026.
16. *Cavaignac J.F., Longequeue N., Honda T.* // Nuclear Phys. A. 1971. V. 167. P. 207. Doi: 10.1016/0375-9474(71)90594-X.

17. *Becker H.W., Rolfs C., Trautvetter H.P.* // Zeitschrift für Physik A. Atomic Nuclei. 1987. V. 327. P. 341. Doi: 10.1007/bf01284459.
18. *Yamashita Y., Kudo Y.* // Nuclear Phys. A. 1995. V. 589. P. 460. Doi: 10.1016/0375-9474(95)00069-D.
19. *Nevins W.M., Swain R.* // Nuclear Fusion. 2000. V. 40. P. 865. Doi: 10.1088/0029-5515/40/4/310.
20. *Sikora M.H., Weller H.R.* // J. Fusion Energ. 2016. V. 35. P. 538. Doi: 10.1007/s10894-016-0069-y.
21. *Tentori A., Belloni F.* // Nuclear Fusion. 2023. V. 63. P. 086001. Doi: 10.1088/1741-4326/acda4b.
22. *Dmitriev V.F.* // Phys. Atomic Nuclei. 2006. V. 69. P. 1461. Doi: 10.1134/S1063778806090043.
23. *Dmitriev V.F.* // Phys. Atomic Nuclei. 2009. V. 72. P. 1165. Doi: 10.1134/S1063778809070084.
24. *Ahmed M.W., Weller H.R.* // J. Fusion Energ. 2014. V. 33. P. 103. Doi: 10.1007/s10894-013-9643-8.
25. *Stave S., Ahmed M.W., France R.H., Henshaw S.S., Müller B., Perdue B.A., Prior R.M., Spraker M.C., Weller H.R.* // Phys. Lett. B. 2011. V. 696. P. 26. Doi: 10.1016/j.physletb.2010.12.015.
26. *Spraker M.C., Ahmed M.W., Blackston M.A., Brown N., France R.H., Henshaw S.S., Perdue B.A., Prior R.M., Seo P.N., Stave S., et al.* // J. Fusion Energ. 2012. V. 31. P. 357. Doi: 10.1007/s10894-011-9473-5.
27. *Belyaev V.S., Krainov V.P., Zagreev B.V., Matafonov A.P.* // Phys. Atomic Nuclei. 2015. V. 78. P. 537. Doi: 10.1134/S1063778815040031.
28. *Belyaev V.S., Matafonov A.P., Vinogradov V.I., Krainov V.P., Lisitsa V.S., Roussetski A.S., Ignatyev G.N., Andrianov V.P.* // Phys. Rev. E. 2005. V. 72. P. 026406. Doi: 10.1103/PhysRevE.72.026406.
29. *Belyaev V.S., Matafonov A.P., Andreev S.N., Tarakanov V.P., Krainov V.P., Lisitsa V.S., Kedrov A.Yu., Zagreev B.V., Rusetskii A.S., Borisenko N.G., Gromov A.I., Lobanov A.V.* // Phys. Atomic Nuclei. 2022. V. 85. P. 31. Doi: 10.1134/S1063778822010070. [*Belyaev V.S., Matafonov A.P., Andreev S.N., Tarakanov V.P., Krainov V.P., Lisitsa V.S., Kedrov A.Yu.,*

Zagreev B.V., Rusetskii A.S., Borisenko N.G., Gromov A.I., Lobanov A.V. // Nuclear Physics. 2022. V. 85. P. 34.]

30. *Labaune C., Baccou C., Depierreux S., Goyon C., Loisel G., Yahia V., Rafelski J.* // Nature Communications. 2013. V. 4. P. 2506. Doi: 10.1038/ncomms3506.
31. *Picciotto A., Margarone D., Velyhan A., Bellutti P., Krasa J., Szydlowsky A., Bertuccio G., Shi Y., Mangione A., Prokupek J., et al.* // Phys. Rev. X. 2014. V. 4. P. 031030. Doi: 10.1103/PhysRevX.4.031030.
32. *Giuffrida L., Belloni F., Margarone D., Petringa G., Milluzzo G., Scuderi V., Velyhan A., Rosinski M., Picciotto A., Kucharik M., et al.* // Phys. Rev. E. 2020. V. 101. P. 013204. Doi: 10.1103/PhysRevE.101.013204.
33. *Margarone D., Morace A., Bonvalet J., Abe Y., Kantarelou V., Raffestin D., Giuffrida L., Nicolai P., Tosca M., Picciotto A., et al.* // Front. Phys. 2020. V. 8. P. 343. Doi: 10.3389/fphy.2020.00343.
34. *Bonvalet J., Nicolaï Ph., Raffestin D., D'humieres E., Batani D., Tikhonchuk V., Kantarelou V., Giuffrida L., Tosca M., Korn G., et al.* // Phys. Rev. E. 2021. V. 103. P. 053202. Doi: 10.1103/PhysRevE.103.053202.
35. *Margarone D., Bonvalet J., Giuffrida L., Morace A., Kantarelou V., Tosca M., Raffestin D., Nicolai P., Picciotto A., Abe Y., et al.* // Appl. Sci. 2022. V. 12. P. 1444. Doi: 10.3390/app12031444.
36. *Istokskaia V., Tosca M., Giuffrida L., Psikal J., Grepl F., Kantarelou V., Stancek S., Di Siena S., Hadjikyriacou A., Mcilvenny A., Levy Y., Huynh J., Cimrman M., Pleskunov P., Nikitin D., Choukourov A., Belloni F., Picciotto A., Kar S., Borghesi M., Lucianetti A., Mocek T., Margarone D* . // Communications Phys. 2023. V. 6. P. 27. Doi: 10.1038/s42005-023-01135-x.
37. *Miley G.H., Hora H.* // Nuclear Fusion. 1998. V. 38. P. 1113. Doi: 10.1088/0029-5515/38/7/413.
38. *Miley G.H., Hora H., Cicchitelli L., Kasotakis G.V., Stening R.J.* // Fusion Technology. 1991. V. 19. P. 43. Doi:10.13182/FST91-A29314.
39. *Hora H., Miley G. H., Ghoranneviss M., Malekynia B., Azizic N., He Xian-Tu*. // Energy Environ. Sci. 2010. V. 3. P. 479. Doi: 10.1039/B904609G.

40. *Eliezer S., Hora H., Korn G., Nissim N., Martinez Val J. M.* // Phys. Plasmas. 2016. V. 23. P. 050704. Doi: 10.1063/1.4950824.
41. *Eliezer S., Martinez-Val J. M.* // Laser Particle Beams. 2022. V. 38. P. 39. Doi: 10.1017/s0263034619000818.
42. *Shmatov M.L.* // Phys. Plasmas. 2016. V. 23. P. 050704; Phys. Plasmas. 2016. V. 23. P. 094703. Doi: 10.1063/1.4963006.
43. *Shmatov M.L.* // Laser Particle Beam 2022. V. 2022. P. 7473118. Doi: 10.1155/2022/7473118.
44. *Belloni F., Margarone D., Picciotto A., Schillaci F., Giuffrida L.* // Phys. Plasmas. 2018. V. 25. P. 020701. Doi: 10.1063/1.5007923.
45. *Belloni F.* // Plasma Phys. Controlled Fusion. 2021. V. 63. P. 055020. Doi: 10.1088/1361-6587/abf255.
46. *Belloni F.* // Laser Particle Beams 2022. V. 2022. P. 3952779. Doi: 10.1155/2022/3952779.
47. *Hora H., Eliezer S., Nissim N., Lalousis P.* // Matter and Radiation at Extremes. 2017. V. 2. P. 177. Doi: 10.1016/j.mre.2017.05.001.
48. *Fujioka S., Zhang Z., Ishihara K., Shigemori K., Hironaka Y., Johzaki T., Sunahara A., Yamamoto N., Nakashima H., Watanabe T., et al.* // Sci. Rep. 2013. V. 3. P. 1170. Doi: 10.1038/srep01170.
49. *Mehlhorn T.A., Labun L., Hegelich B. M., Margarone D., Gu M. F., Batani D., Campbell E. M., Hu S.X.* // Laser Particle Beams. 2022. V. 2022. P. 2355629. Doi: 10.1155/2022/2355629.
50. *Ribeyre X., Capdessus R., Wheeler J., d'Humières E., Mourou G.* // Sci. Reps. 2022. V. 12. P. 4665. Doi: 10.1038/s41598-022-08433-4.
51. *Belyaev V.S., Vinogradov V.I., Matafonov A.P., Rybakov S.M., Krainov V.P., Lisitsa V.S., Andrianov V.P., Ignatiev G.N., Bushuev V.S., Gromov A.I., Rusetsky A.S., Dravin V.A.* // Phys. Atomic Nuclei. 2009. V. 72. P. 1077. Doi: 10.1134/S1063778809070011.
52. *Guskov S.Yu., Korneev F.A.* // JETP Lett. 2016. V. 104. P. 1. Doi: 10.1134/S0021364016130117.
53. *Andreev S. N., Matafonov A. P., Tarakanov V. P., Belyaev V. S., Kedrov A. Yu., Krainov V. P., Mukhanov S. A., Lobanov A.V.* // Phys. Atomic Nuclei. 2023. V. 86. P. 406. Doi: 10.1134/S1063778823040038.

54. *Dubinov A.E., Kornilova I.Yu., Selemir V.D.* // Physics-Uspekhi. 2002. V. 172. P. 1225. Doi: 10.3367/UFNr.0172.200211a.1225.

55. *Macchi A., Borghesi M., Passoni M.* // Rev. Mod. Phys. 2013. V. 85. P. 751. Doi: 10.1103/RevModPhys.85.751.

56. *Bychenkov V.Yu., Brantov A.V., Govras E.A., Kovalev V.F.* // Physics-Uspekhi. 2015. V. 185. P. 77. Doi: 10.3367/UFNr.0185.201501f.0077.

57. *Magee R.M., Ogawa K., Tajima T., Allfrey I., Gota H., McCarroll P., Ohdachi S., Isobe M., Kamio S., Klumper V., et al.* // Nature Commun. 2023. V. 14. P. 955. Doi: 10.1038/s41467-023-36655-1.

58. *Rostoker N., Binderbauer M.W., Monkhorst H.J.* // Science. 1997. V. 278. P. 1419. Doi: 10.1126/science.278.5342.1419.

59. *Volosov V.I.* // Nuclear Fusion. 2006. V. 46. P. 820. Doi: 10.1088/0029-5515/46/8/007.

60. *Nevins W.M.* // Science. 1998. V. 281. P. 307. Doi: 10.1126/science.281.5375.307a.

61. *Moustaizis S., Daponta C., Eliezer S., Henis Z., Lalousis P., Nissim N., Schweitzer Y.* // J. Instrumentation. 2024. V. 19. P. C01015. Doi: 10.1088/1748-0221/19/01/C01015.

62. *Bone T., Sedwick R.* // Acta Astronautica. 2024. V. 220. P. 356. Doi: 10.1016/j.actaastro.2024.04.040.

63. *Liu M., Xie H., Wang Y., Dong J., Feng K., Gu X., Huang X., Jiang X., Li Y., Li Z., et al.* // Phys. Plasmas. 2024. V. 31. P. 062507. Doi: 10.1063/5.0199112.

64. *Rider T.H.* // Phys. Plasmas. 1995. V. 2. P. 1853. Doi: 10.1063/1.871273.

65. *Kurilenkov Yu. K., Oginov A. V., Tarakanov V. P., Guskov S. Yu., Samoylov I. S.* // Phys. Rev. E. 2021. V. 103. P. 043208. Doi: 10.1103/PhysRevE.103.043208.

66. *Kurilenkov Yu. K., Tarakanov V. P., Oginov A. V., Guskov S. Yu., Samoylov I. S.* // Laser Particle Beams. 2023. V. 2023. P. 9563197. Doi: 10.1155/2023/9563197.

67. *Wong A.Y., Shih C.C.* // Plasma. 2022. V. 5. P. 176. Doi: 10.3390/plasma5010013.

68. *Hurricane O.A., Callahan D.A., Casey D.T., Celliers P.M., Cerjan C., Dewald E.L., Dittrich T.R., Döppner T., Hinkel D.E., Hopkins L.F.B., et al.* // Nature. 2014. V. 506. P. 343. Doi: 10.1038/nature13008.

69. *Yager-Elorriaga D.A., Gomez M.R., Ruiz D.E., Slutz S.A., Harvey-Thompson A.J., Jennings C.A., Knapp P.F., Schmit P.F., Weis M.R., Awe T.J., et al.* // Nuclear Fusion. 2022. V. 62. P. 042015. Doi: 10.1088/1741-4326/ac2dbe.

70. *Garanin S.F*. Physical Processes in MAGO-MTF Systems. Sarov: RFNC-VNIIEF, 2012.
71. *Ghorbanpour E., Belloni F*. // Front. Phys. 2024. V. 12. P. 1405435. Doi: 10.3389/fphy.2024.1405435.
72. *G horbanpour E., G hasemizad A., K hoshbinfar S*. // Phys. Particles Nuclei Lett. 2020. V. 17. P. 809. Doi: 10.1134/S1547477120060126.
73. *Mahdavi M., Bakhtiyari M., Najafi A*. // Internat. J. Mod. Phys. B. 2023. V. 37. P. 2350142. Doi: 10.1142/S0217979223501424.
74. *Khademloo E., Mahdavi M., Azadboni F.K*. // Indian J Phys. 2024. V. 98. P. 4543. Doi: 10.1007/s12648-024-03193-5.
75. *Auluck S., Kubes P., Paduch M., Sadowski M.J., Krauz V.I., Lee S., Soto L., Scholz M., Miklaszewski R., Schmidt H., et al*. // Plasma. 2021. V. 4. P. 450. Doi: 10.3390/plasma4030033.
76. *Haruki T., Yousefi H. R., Sakai J.I.* // Phys. Plasmas. 2010. V. 17. P. 032504. Doi: 10.1063/1.3318470.
77. *Abolhasani S., Habibi M., Amrollahi R*. // J. Fusion. Energ. 2013. V. 32. P. 189. Doi: 10.1007/s10894-012-9547-z.
78. *Di Vita A*. // European Phys. J. 2013. V. 67. P. 191. Doi: 10.1140/epjd/e2013-40096-3.
79. *Scholz M., Kro´ K., Kulin A., Karpin L., Wo´jcik-Gargula A., Fitta M*. // J. Fusion Energy. 2019. V. 38. P. 522. Doi: 0.1007/s10894-019-00225-5.
80. *Lerner E. J., Hassan S. M., Karamitsos-Zivkovic I., Fritsch R*. // J. Fusion Energy. 2023. V. 42. P. 7. Doi: 10.1007/s10894-023-00348-w; Correction // J. Fusion Energy. 2023. V. 42. P. 9. Doi: 10.1007/s10894-023-00348-w.
81. *Vikhrev V.V., Korolev V.D*. // Plasma Phys. Rep. 2007. V. 33. P. 356. Doi: 10.1134/S1063780X07050029.
82. *Akel M., AL-Hawat S., Ahmad M., Ballul Y., Shaaban S*. // Plasma. 2022. V. 5. P. 184. Doi: 10.3390/plasma5020014.
83. *Shumlak U*. // J. Appl. Phys. 2020. V. 127. P. 200901. Doi: 10.1063/5.0004228.
84. *Shumlak U., Meier E. T., Levitt B. J.* // Fusion Sci. Technol. 2024. V. 80. P. 1. Doi: 10.1080/15361055.2023.2198049.
85. *Pikuz S. A., Sinars D. B., Shelkovenko T. A., Chandler K. M., Hammer D.A., Ivanenkov G.V., Stepniewski W., Skobelev I.Yu*. // Phys. Rev. Lett. 2024. V. 89. P. 035003. Doi: 10.1103/PhysRevLett.89.035003.

86. *Kroupp E., Stambulchik E., Starobinets, A., Osin D., Fisher V.I., Alumot D., Maron Y., Davidovits S., Fisch N. J., Fruchtman A*. // Phys. Rev. E. 2018. V. 97. P. 013202. Doi: 10.1103/PhysRevE.97.013202.

87. *Davidovits S., Kroupp E., Stambulchik E., Maron Y*. // Phys. Rev. E. 2021. V. 103. P. 063204. Doi: 10.1103/PhysRevE.103.063204.

88. *Vikhrev V.V., Frolov A.Yu., Chirkov A.Yu* . // J. Physics: Confer. Ser. 2019. V. 1370. P. 012026. Doi: 10.1088/1742-6596/1370/1/012026

89. *Chirkov A.Yu., Tokarev S. A*. // Fusion Sci. Technology. 2023. V. 79. P. 413. Doi: 10.1080/15361055.2022.2135337.

90. *Son S., Fisch N.J.* // Phys. Lett. A. 2004. V. 329. P. 76. Doi: 10.1016/j.physleta.2004.06.054.

91. *Hosseini Motlagh S.N., Mohamadi Sh.S., Shamsi R*. // J Fusion Energy. 2008. V. 27. P. 161. Doi: 10.1007/s10894-007-9124-z.

92. *Eliezer S., León P.T., Martinez-Val J.M., Fisher D.V*. // Laser Particle Beams. 2003. V. 21. P. 599. Doi: 10.10170S0263034603214191.

93. *Dzhavakhishvili D.I., Tsintsadze N.L*. // Sov. Phys.— JETP. 1973. V. 37. P. 666. Doi: 10.1088/1741-4326/acee96.

94. *Lavrinenko Y.S., Morozov I.V., Valuev I.A*. // Contrib. Plasma Phys. 2024. V. 64. P. e202300158. Doi: 10.1002/ctpp.202300158.

95. *Svensson R*. // Astrophys. J. 1982. V. 258. P. 335. Doi: 10.1086/160082.

96. *Li Z.* // Phys. Plasmas. 2024. V. 31. P. 084701. Doi: 10.1063/5.0223575.

97. *Basko M.M*. // Nucl. Fusion. 1990. V. 30. P. 2443. Doi: 10.1088/0029-5515/30/12/001.

98. *Zeldovich Ya.B., Raizer Yu.P* . Physics of Shock Waves and High-Temperature Hydrodynamic Phenomena. Moscow: Nauka, 1966. [Zeldovich Ya.B., Raizer Yu.P. *Physics of Shock Waves and High-Temperature Hydrodynamic Phenomena* (Academic Press, New York–London, 1966).]

99. *Moseev D., Salewski M*. // Phys. Plasmas. 2019. V. 26. P. 020901. Doi: 10.1063/1.5085429.

100. *Xie H., Tan M., Luo D., Li Z., Bing L*. // Plasma Phys. Control. Fusion. 2023. V. 65. P. 055019. Doi: 10.1088/1361-6587/acc8f9.

101. *Kong H., Xie H., Bing L., Tan M., Luo D., Li Z., Sun J.* // Plasma Phys. Control. Fusion. 2024. V. 66. P. 015009. Doi: 10.1088/1361-6587/ad1008.

102. *Binderbauer M. W., Rostoker N.* // J. Plasma Phys. 1996. V. 56. P. 451. Doi: 10.1017/S0022377800019413.

103. *Tchórz P., Chodukowski T., Rosiński M., Borodziuk S., Szymański M., Dudžák R., Singh S., Krupka M., Burian T., Marchenko A., et al.* // Phys. Plasmas. 2024. V. 31. P. 084503. Doi:10.1063/5.0207108.

104. *Putvinskii S.V.* // Reviews of Plasma Physics. V. 18 / Ed. B.B. Kadomtsev. 1993. P. 239.

105. *Zhang D., Wang X., Dong C., Bao J., Cao J., Zhang W., Li D.* // Phys. Plasmas. 2024. V. 31. P. 042509. Doi: 10.1063/5.0197259.

106. *Baldwin D.E., Byers J.A., Chen Y.J., Kaiser T.B.* // IAEA Internat. Confer. on Plasma Phys. Controlled Nuclear Fusion Research. Kyoto. Japan. 12 November 1986. IAEA. Vienna. Austria. 1986. P. 293.

107. *Shabrov N.V., Khvesjuk V.I.* // Fusion Technology. 1994. V. 26. P. 117. Doi: 10.13182/FST94-A30335.

108. *Khvesyuk V.I., Shabrov N.V., Lyakhov A.N.* // Fusion Technol. 1995. V. 27 P. 406. Doi: 10.13182/FST95-A11947116.

109. Gudinetsky E., Miller T., Be'ery I., Barth I. // arXiv.2402.18687. 2024. Doi: 10.48550/arXiv.2402.18687.

110. *Barth I., Friedland L., Sarid E., Shagalov A.G.* // Phys. Rev. Lett. 2009. V. 103. P. 155001. Doi: 10.1103/PhysRevLett.103.155001.

111. *Munirov V.R., Fisch N.J.* // Phys. Rev. E. 2023. V. 107. P. 065205. Doi: 10.1103/PhysRevE.107.065205.

112. *Ochs I.E., Mlodik M.E., Fisch N.J.* // Phys. Plasmas. 2024. V. 31. P. 083303. Doi: 10.1063/5.0228464.

Table 1. Main parameters of laser systems and characteristics of α-particle spectrum.

Facility; Laboratory, Location	Year [reference]	Parameters	Alpha-particle yield, spectrum features
"Neodymium"; Korolev, Russia	2005 [28]	$\lambda = 1.055$ μm, $E = 15$ J, $I = 2 \cdot 10^{18}$ W/cm^2, $\tau = 1.5$ ps	$1.3 \cdot 10^5$ sr^{-1} α: 2–10 MeV max at 3–4 MeV (α_{12}) max at 6–10 MeV (α_1)
	2022 [29]	$\lambda = 1.055$ μm, $E = 10$ J, $I = 3 \cdot 10^{18}$ W/cm^2, $\tau = 1.5$ ps	10^8 sr^{-1} per pulse α: 0.5–4.5 MeV
Pico2000; LULI, France	2013 [30]	1st beam: $\lambda = 0.53$ μm, $E = 400$ J, $I = 5 \cdot 10^{14}$ W/cm^2, $\tau = 4$ ns; 2nd beam: $\lambda = 0.53$ μm, $E = 20$ J, $I = 6 \cdot 10^{18}$ W/cm^2, $\tau = 1.5$ ps, $n_e = 6 \cdot 10^{23}$ cm^{-3}	$9 \cdot 10^6$ sr^{-1} α: 3–8 MeV max at 3.5 MeV
PALS; Prague, Czech Republic	2014 [31]	$\lambda = 1.315$ μm 1st pulse: $E = 50$ J, $I = 3 \cdot 10^{10}$ W/cm^2, $\tau = 1$ ns; 2nd pulse: $E = 100$ J, $I = 1 \cdot 10^{15}$ W/cm^2, $\tau = 1$ ns; 3rd pulse: $E = 50$ J, $I = 3 \cdot 10^{16}$ W/cm^2, $\tau = 0.3$ ns	$1 \cdot 10^9$ sr^{-1} α_1: 3–8 MeV, max at 4.6 MeV α_2: 7–11 MeV max at 8.9 MeV
	2020 [32]	$\lambda = 1.315$ μm, $E = 600$ J, $\tau = 0.3$ ns, $I = 3 \cdot 10^{16}$ W/cm^2	$1.3 \cdot 10^{11}$ sr^{-1} α: 2.6–10 MeV max at 3.5 MeV
LFEX; Osaka, Japan	2020 [33]	$\lambda = 1.315$ μm, $E = 600$ J, $\tau = 0.3$ ns, $I = 3 \cdot 10^{16}$ W/cm^2	$5 \cdot 10^9$ sr^{-1} α: 8–10 MeV max at 8.6 MeV
	2021 [34] 2022 [35]	$\lambda = 1.05$ μm, $E = 1.4$ kJ, $I = (2–3) \cdot 10^{19}$ W/cm^2, $\tau = 2.6$ ps	$1.2 \cdot 10^{10}$ sr^{-1} α: 5–10 MeV max at 5 MeV
PERLA B; HiLASE Center, Czech Republic	2023 [36]	$E = 10$ mJ, $\tau = 1.5$ ps, $I = (2–3) \cdot 10^{16}$ W/cm^2, $n_B = 5 \cdot 10^{19}$ cm^{-3}	$6 \cdot 10^4$ s^{-1} at 10 Hz $1 \cdot 10^6$ s^{-1} at 1 kHz α: 1–4.5 MeV,

			max at 3.5 MeV

FIGURE CAPTIONS

Рис. 1. Reaction scheme: ^{12}C* — compound nucleus (p + ^{11}B), α — alpha particle, $\mathbf{p}_1$ and $\mathbf{p}_2$ denote alpha particle momenta.

Рис. 2. Energy spectrum of alpha particles calculated in [23].

Рис. 3. Cross-section dependence of p-^{11}B reaction on collision energy according to "new" [21] (solid line) and "old" [19] (dashed line) data.

Рис. 4. Dependence of reaction rate parameter on ion temperature T_i: *1* - dependence obtained by numerical integration of cross-section from [19], *2* - by formula from [19], *3* , *4* - dependencies according to [21] (results of numerical integration of cross-section and calculation by formula practically coincide).

Рис. 5. Reaction rate parameter of p-^{11}B versus ion temperature T_i at different energies of relative motion of components (E - energy in center-of-mass system).

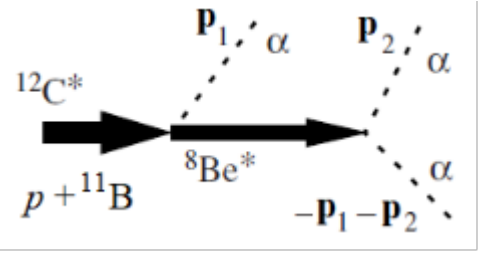

Fig. 1.

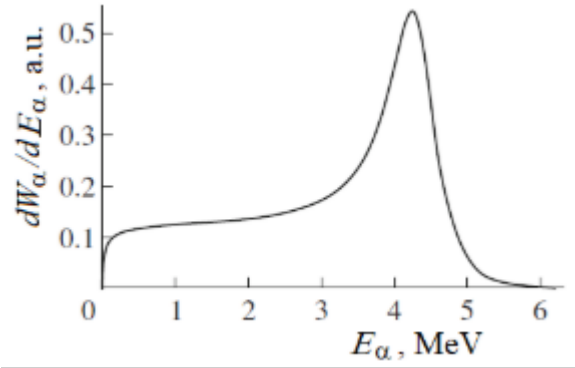

Fig. 2.

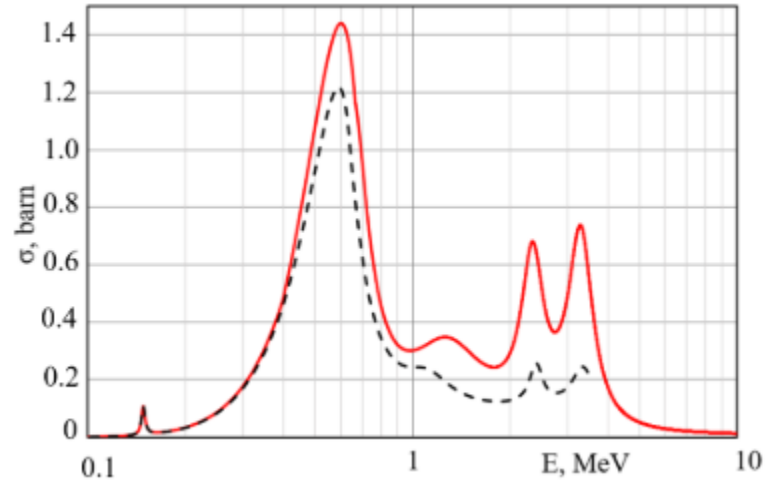

Fig. 3.

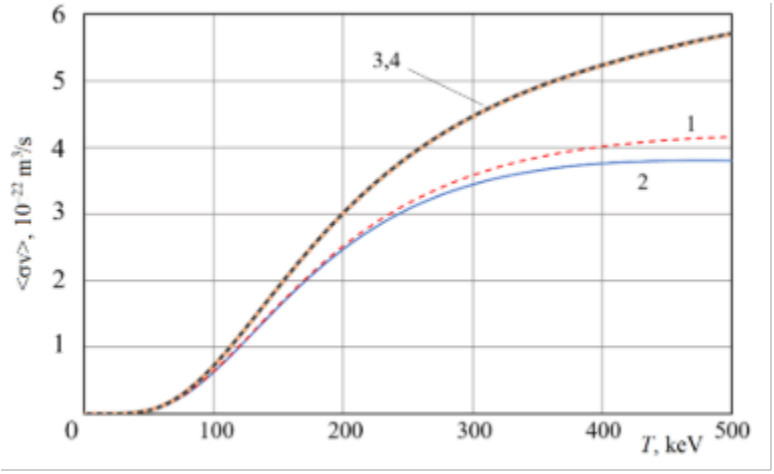
6
5
4
3
2
1
0
100
200
300
400
500
T, keV
<σv>, 10⁻²² m³/s
3,4
1
2

Fig. 4.

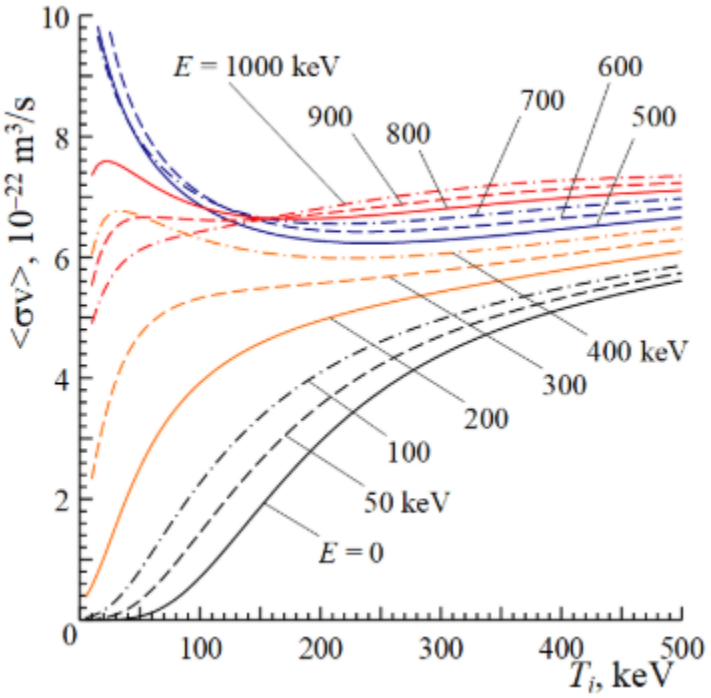
10
8
6
4
2
0
100
200
300
400
500
T_i, keV
<σv>, 10⁻²² m³/s
E = 1000 keV
900
800
700
600
500
400 keV
300
200
100
50 keV
E = 0

Fig. 5.